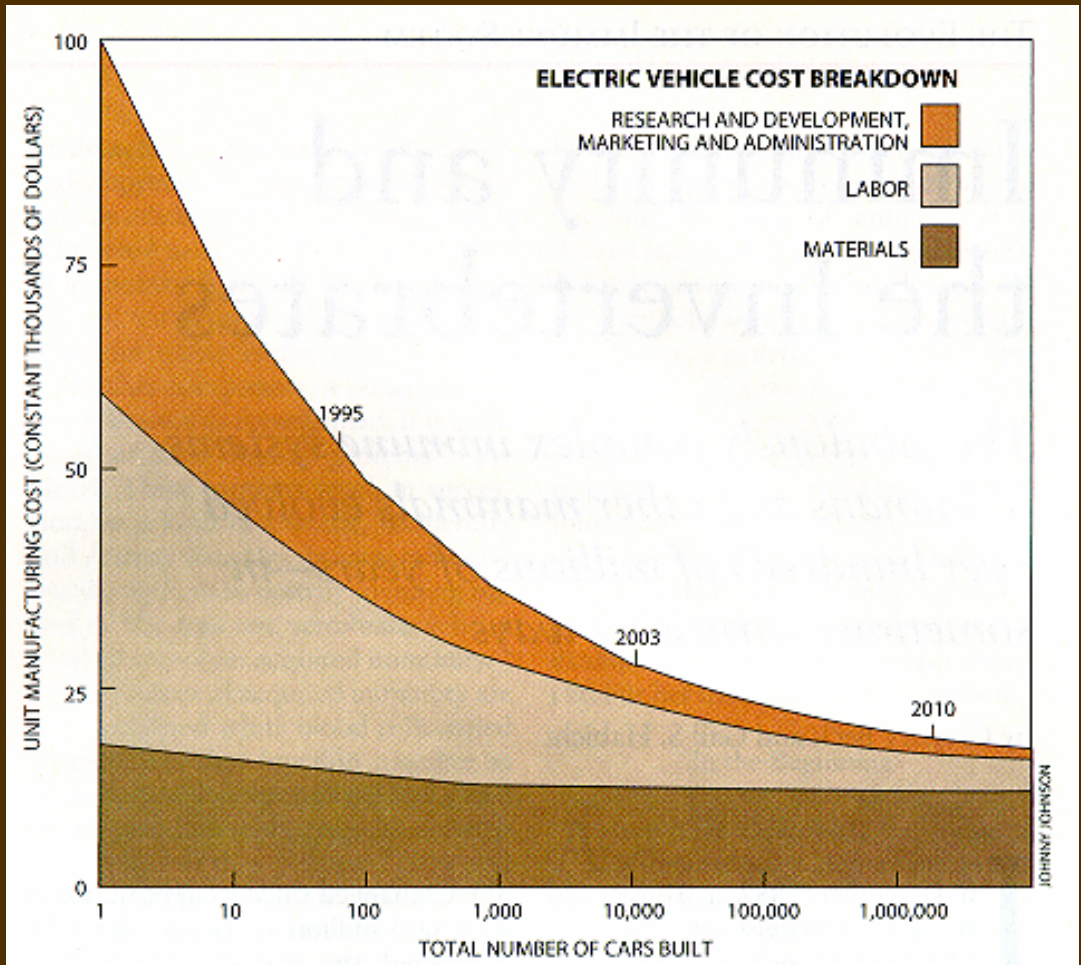

ECONOMIES OF SCALE should enable manufacturers to reduce the prices of electric vehicles once production volumes increase beyond their current level of a few vehicles a day. Eventually the cost of materials will dominate the total cost of electric vehicles. (These estimates are derived from experience with conventional vehicle manufacturing, in which a typical factory produces 100,000 or more vehicles a year.)

Custos unitários de fabricação de veículos elétricos.
Obs.: ln (preço de materiais poliméricos) é função linear de ln(escala)

Electric Vehicles Reduce Pollution

(Percentage Change in Emissions)

FRANCE	–99	–99	–91	–58	–59
GERMANY	–98	–99	–66	+96	–96
JAPAN	–99	–99	–66	–40	+10
U.K.	–98	–99	–34	+407	+165
U.S.	–96	–99	–67	+203	+122
CALIFORNIA	–96	–97	–75	–24	+15

JOHNSON JOHNSON

SOURCES: Choosing an Alternative Fuel: Air Pollution and Greenhouse Gas Impacts *(OECD, Paris, 1993). U.S. estimates are from Q. Wang, M. DeLuchi and D. Sperling, "Emission Impacts of Electric Vehicles," Journal of the Air and Waste Management Association, Vol. 40, No. 9, pages 1275–1284; September 1990.*

BATTERY-POWERED electric cars, if they were accepted universally, would slash production of major urban pollutants, according to simulations. Pollution from power plants, however, would in some cases partially offset these gains or even increase certain kinds of pollution, especially in countries (such as the U.K. and the U.S.) that rely heavily on coal and oil.

Sperling em Sci. Am., 96

Redução de peso em automóveis elétricos: 60% nos componentes eletro-eletrônicos (verde, atual; cinzento, anterior)

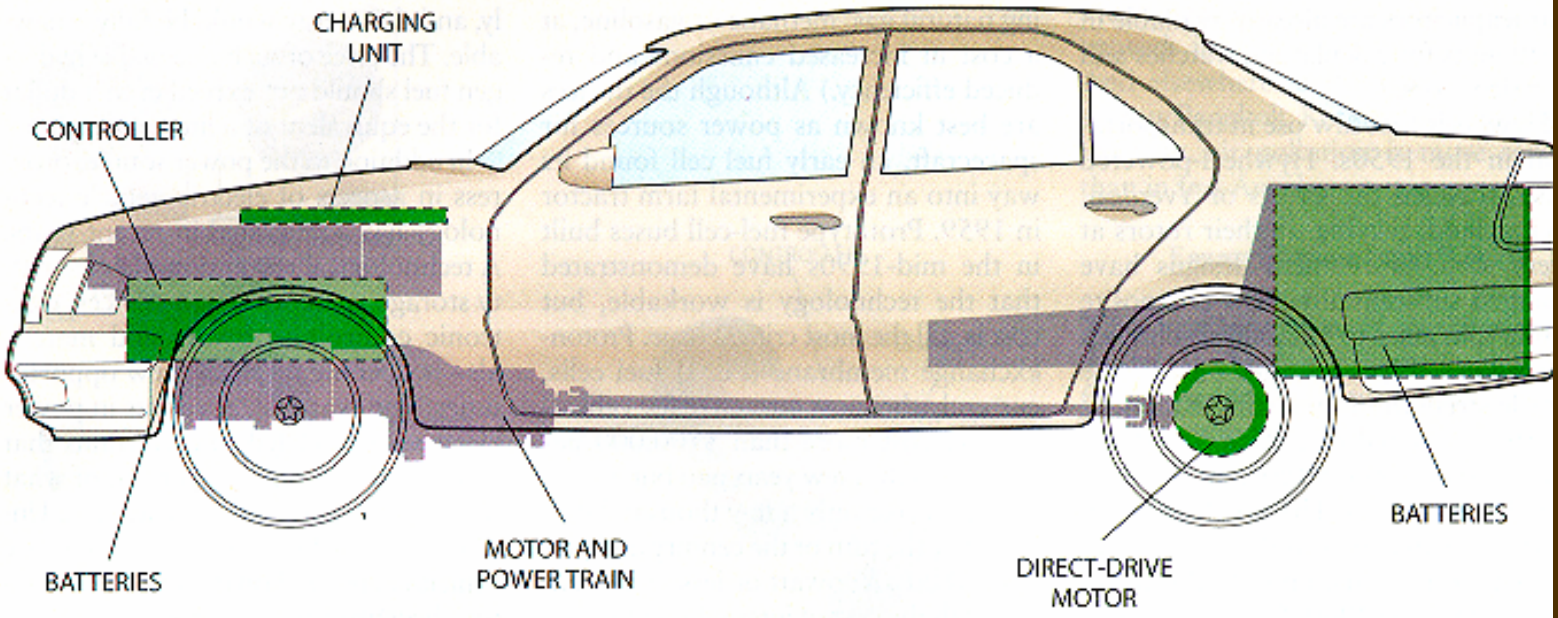

MINIATURIZATION of electronics and advances in batteries and motors have cut the weight of electric-vehicle storage cells and drive components by as much as 60 percent during the past 10 years (older devices are shown in gray in the schematic above, newer ones in dark green and the overlap in light green). Tl reduction has in turn decreased the weight required for the ca suspension and structural components, making it possible achieve equivalent performance with even smaller component

Reciclagem é parte essencial no ***ciclo de vida*** de qualquer material. A motivação é econômica e ambiental

Polímeros nov/dez 96

Exemplo de uma Linha Completa para Reciclagem Mecânica de Resíduos Plásticos

(Ilustração Cedida pela Empresa KIE Máquinas Ltda)

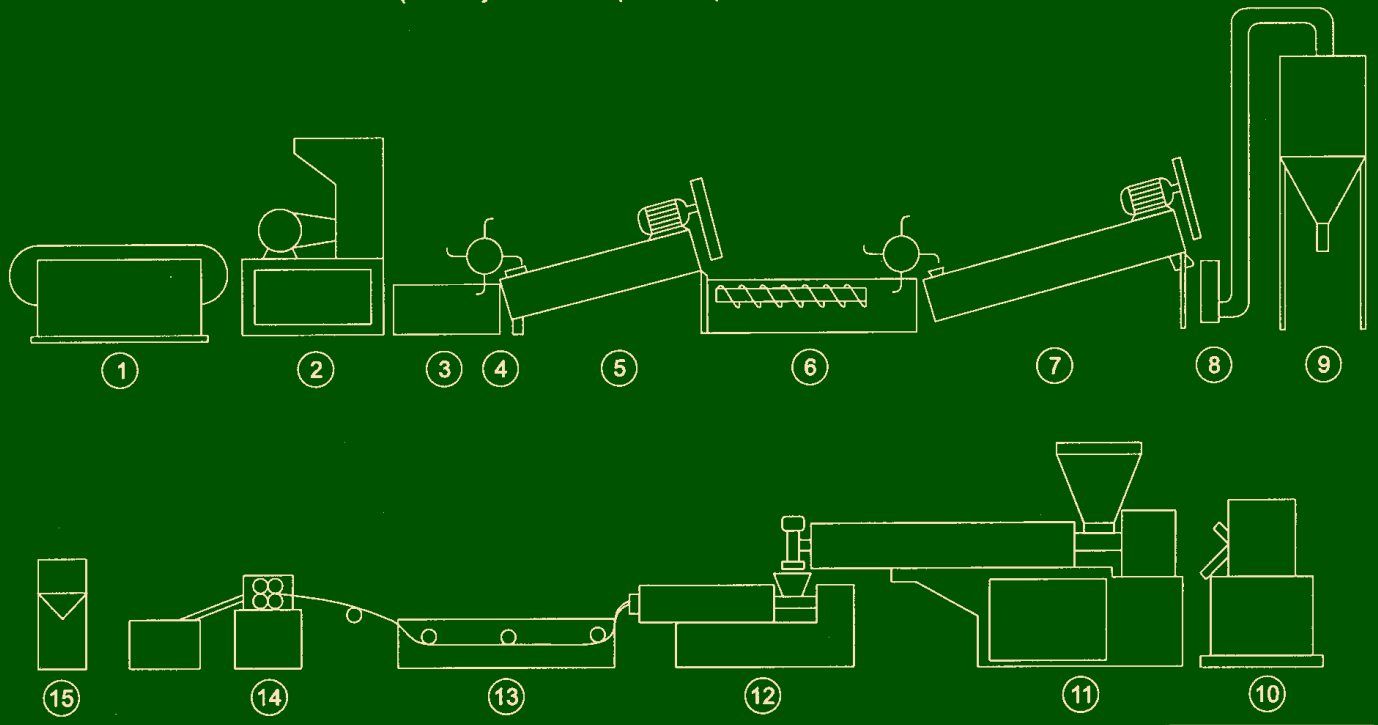

1 Esteira Transportadora
2 Moinho
3 Gadanho
4 Roda Transportadora
5 Lavadora
6 Rosca Transportadora
7 Secadora
8 Ventoinha
9 Silo
10 Aglutinador
11 Extrusora 1
12 Extrusora 2
13 Banheira
14 Granulador
15 Ensacador

Injeção (com tolerâncias de 10 μm ou menos, várias peças por minuto) vs. usinagem

B. Webb, "A Cricket Robot", Sci. Am. 96

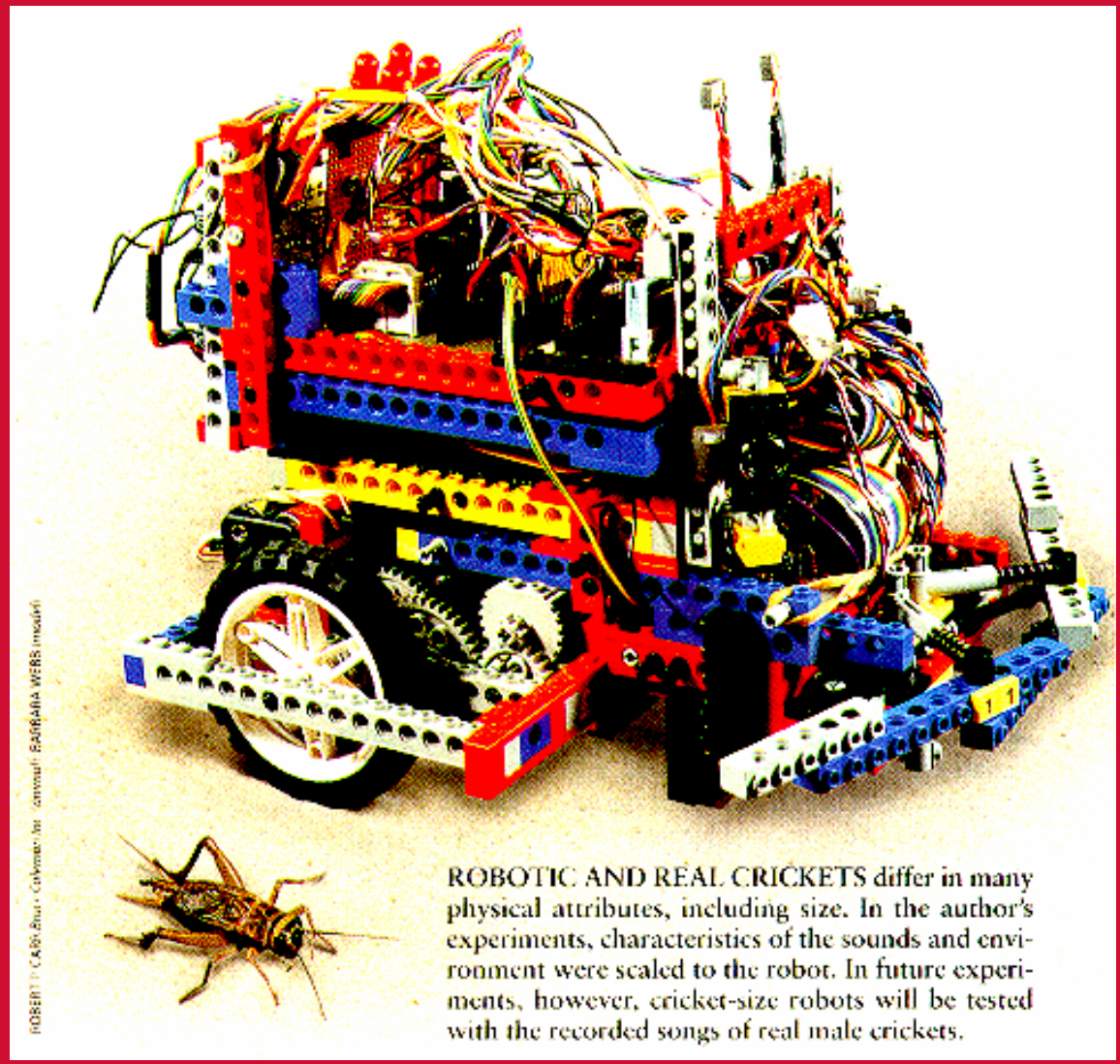

ROBOTIC AND REAL CRICKETS differ in many physical attributes, including size. In the author's experiments, characteristics of the sounds and environment were scaled to the robot. In future experiments, however, cricket-size robots will be tested with the recorded songs of real male crickets.

Processamento reativo: soldagem ($B+C+Al+Ni+SiO_2$, folhas fabricadas por sputtering)

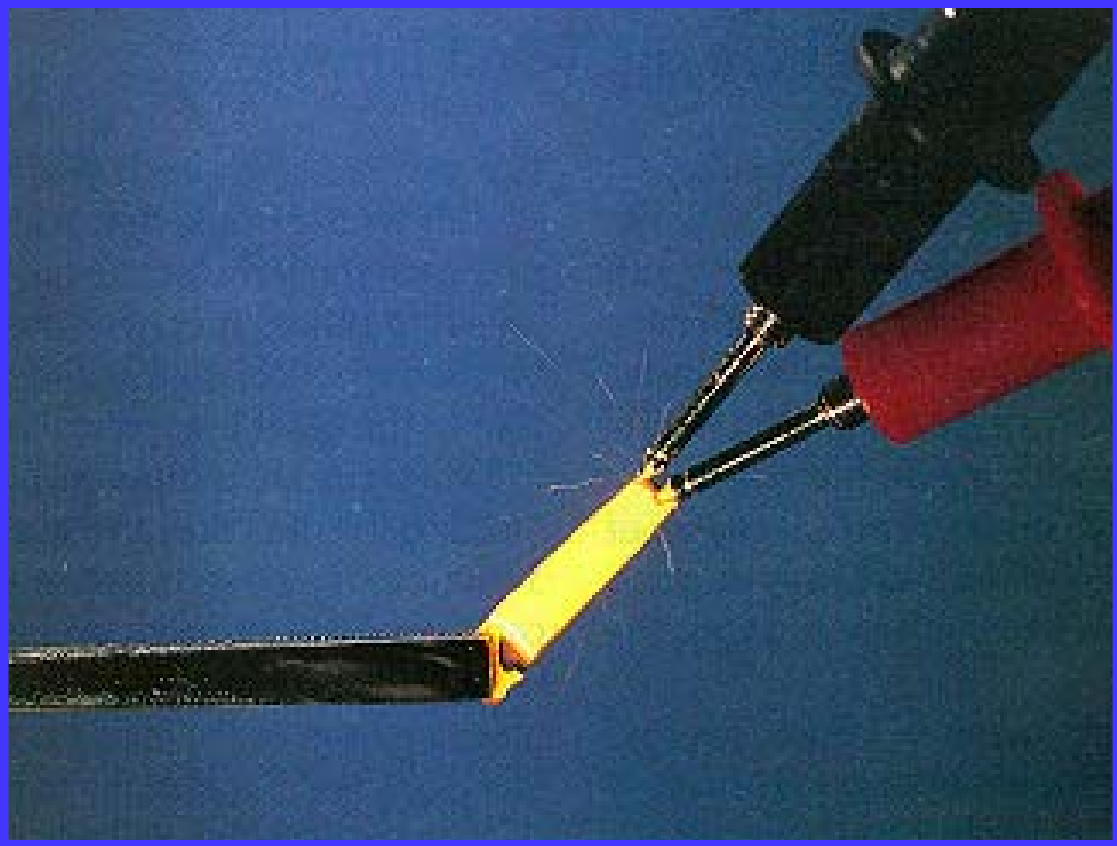

Barbie, Weihs, pat.

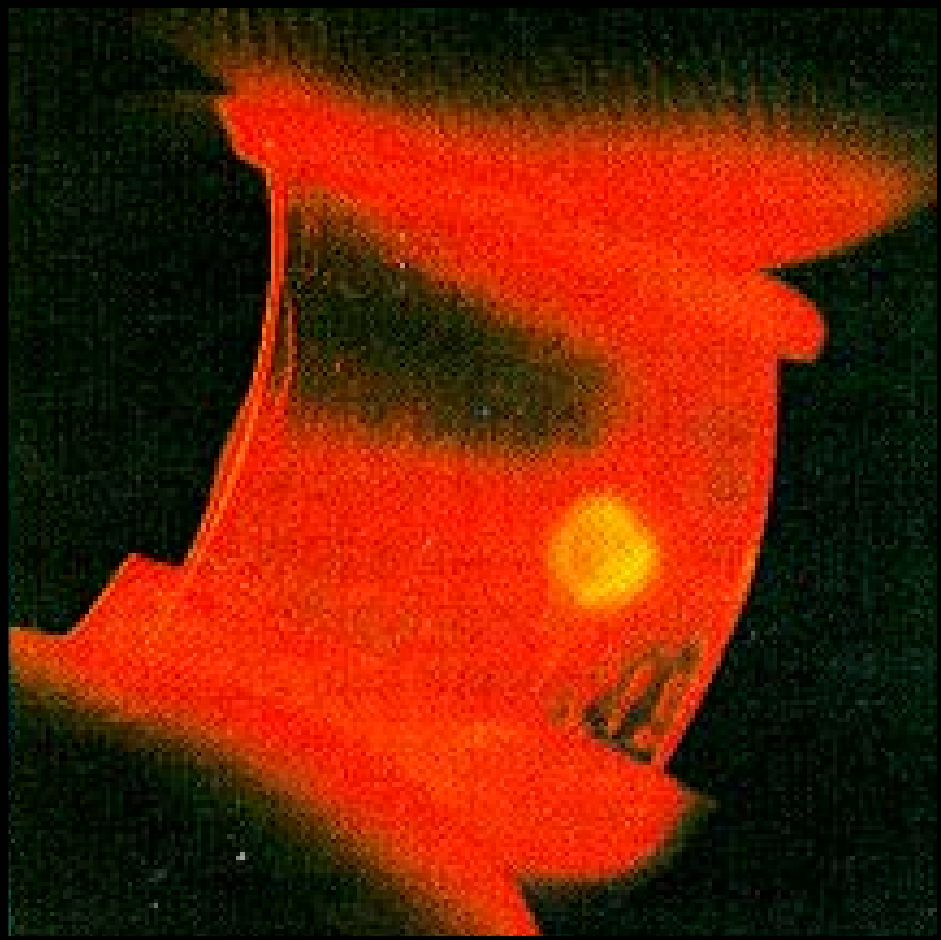

POLÍMEROS CONDUTORES

PPV (poli para-fenilenovinileno) luminescente: laser de polímero?

e mais: células solares de PVA/PA (Lumeloid): 75% de rendimento, 50 cents (por watt)

Potential Biological Agents

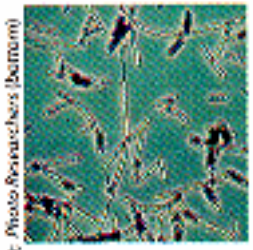

Bacillus anthracis. Causes anthrax. If bacteria are inhaled, symptoms may develop in two to three days. Initial symptoms resembling common respiratory infection are followed by high fever, vomiting, joint ache and labored breathing, and internal and external bleeding lesions. Exposure may be fatal. Vaccine and antibiotics provide protection unless exposure is very high.

Botulinum toxin. Cause of botulism, produced by *Clostridium botulinum* bacteria. Symptoms appear 12 to 72 hours after ingestion or inhalation. Initial symptoms are nausea and diarrhea, followed by weakness, dizziness and respiratory paralysis, often leading to death. Antitoxin can sometimes arrest the process.

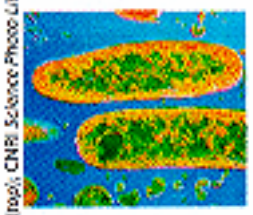

Yersinia pestis. Causes bubonic plague, the Black Death of the Middle Ages. If bacteria reach the lungs, symptoms—including fever and delirium—may appear in three or four days. Untreated cases are nearly always fatal. Vaccines can offer immunity, and antibiotics are usually effective if administered promptly.

Ebola virus. Highly contagious and lethal. May not be desirable as a biological agent because of uncertain stability outside of animal host. Symptoms, appearing two or three days after exposure, include high fever, delirium, severe joint pain, bleeding from body orifices, and convulsions, followed by death. No known treatment.

M. WALKER (Photo Researchers Inc.); CNRI (Science Photo Library)/Photo Researchers (microbe text); Photo Researchers (bottom)

"Se é químico é danoso, se é biológico é natural e saudável" ??????

Cole, "The specter of biological weapons"

4 ns

7.5 μs

350 μs

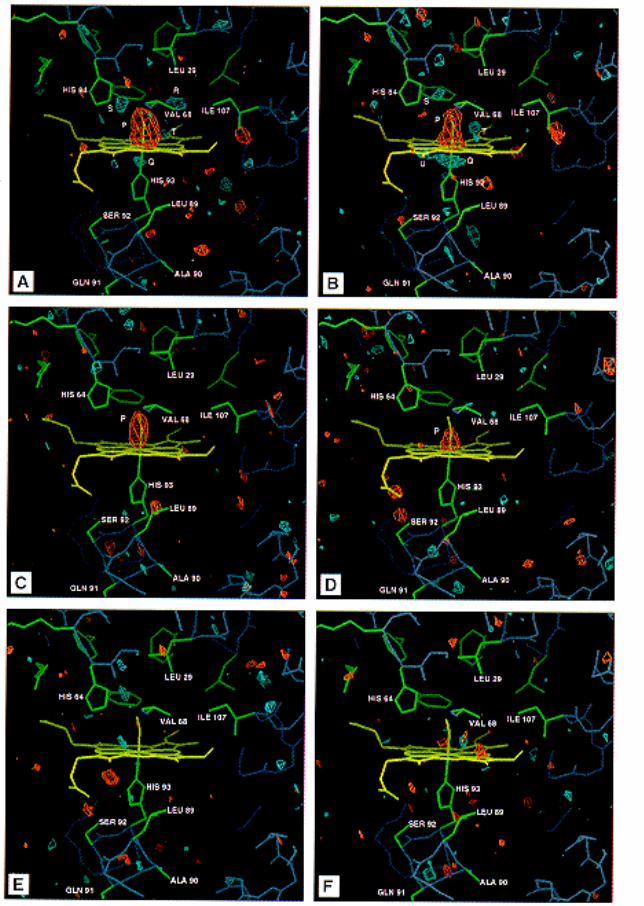

Fig. 1. Difference Fourier maps of the heme region, at different time delays after the laser pulse. The maps are calculated at 1.5 Å resolution with structure factor amplitudes $\Delta F = \{|F(\mathrm{Mb}^*(t))| - |F(\mathrm{MbCO})|\}$ obtained from the combined single and multiple reflections (Table 1) and calculated phases (25). The model of MbCO is also shown. The difference Fourier coefficients are weighted by a factor of $w/\langle w \rangle$, where $w = \sigma^2/(\sigma^2 + 2\sigma^2\langle\Delta F\rangle)$, σ is the standard deviation of the ΔF distribution as a function of resolution, $\sigma^2(\Delta F) = \sigma^2(F, \mathrm{MbCO}) + \sigma^2(F, \mathrm{Mb}^*)$, and $\langle w \rangle$ is the mean value of w. The factor of 2 scales $\sigma^2(\Delta F)$ to σ^2 since the values of $\sigma(\Delta F)$ are somewhat underestimated. Maps are contoured at $\pm 3\sigma$ (0.12 e/Å^3) where σ is the root-mean-square (rms) value of the difference density over the asymmetric unit. Negative contours are shown in red and positive in blue. (**A**) Four-nanosecond time delay after CO photodissociation; (**B**) 1-μs delay; (**C**) 7.5-μs delay; (**D**) 50.5-μs delay; (**E**) 350-μs delay; (**F**) 1.9-ms delay; (**G**) the corresponding, reference difference Fourier map calculated from deoxy Mb (24) and MbCO (25) models with reflections identical to those in the 4-ns time delay x-ray data.

Cristalografia resolvida no tempo: fotólise de CO-mioglobina

Srajer, Teng, Moffat et al., *Science 96*

(irradiado na European Synchrotron Radiation Facility)

Nanotubos de carbono: Tibbetts descobriu fibras ocas de C, formadas por difusão de Fe em C ou por pirólise de CH_4 sobre ferro; Li et al. sintetizam nanotubos em larga escala, usando nanopartículas de Fe.

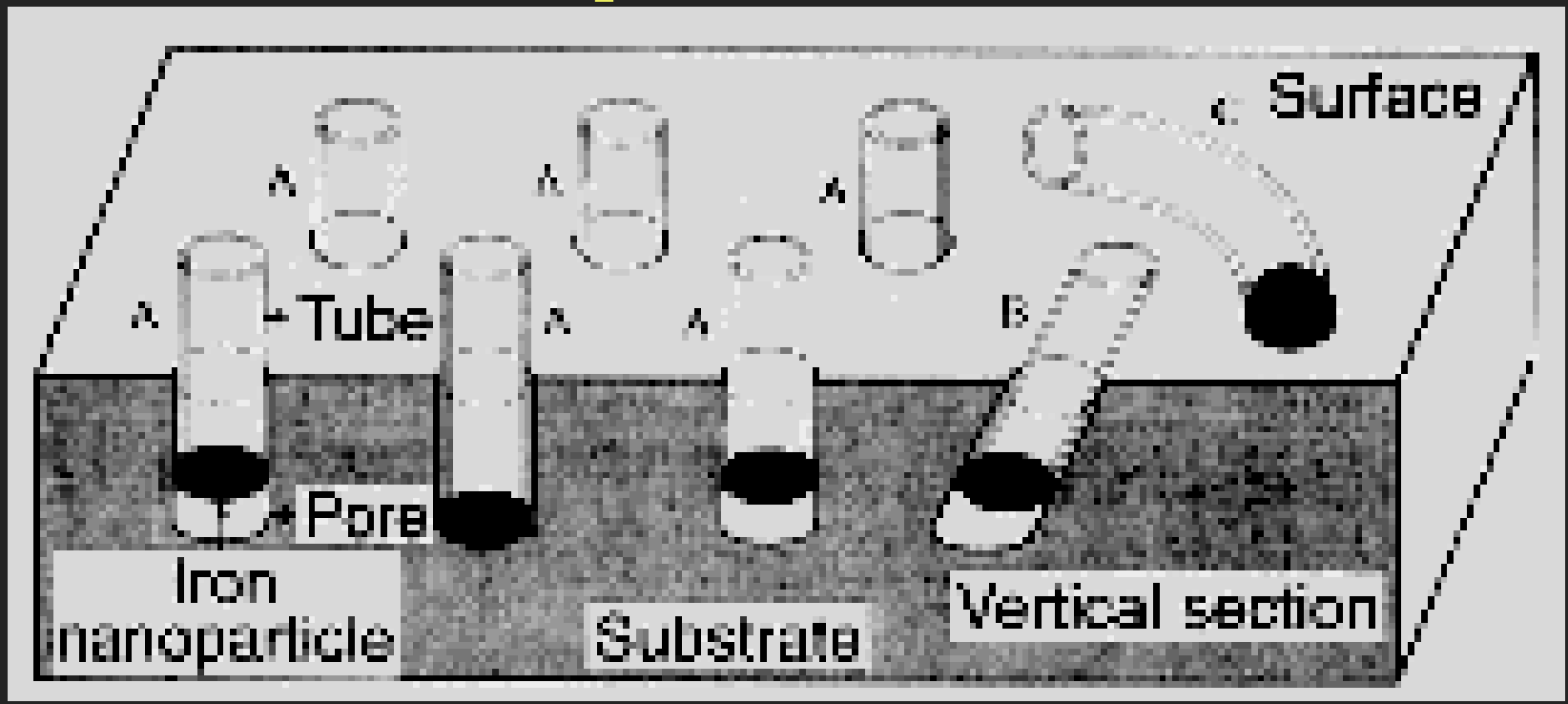

Espectroscopia de raios-X resolvida no tempo: V^{5+} decai proporcionalmente à taxa de formação de anidrido maleico, na oxidação de butano catalisada por fosfatos de vanádio (Coulston, 97)

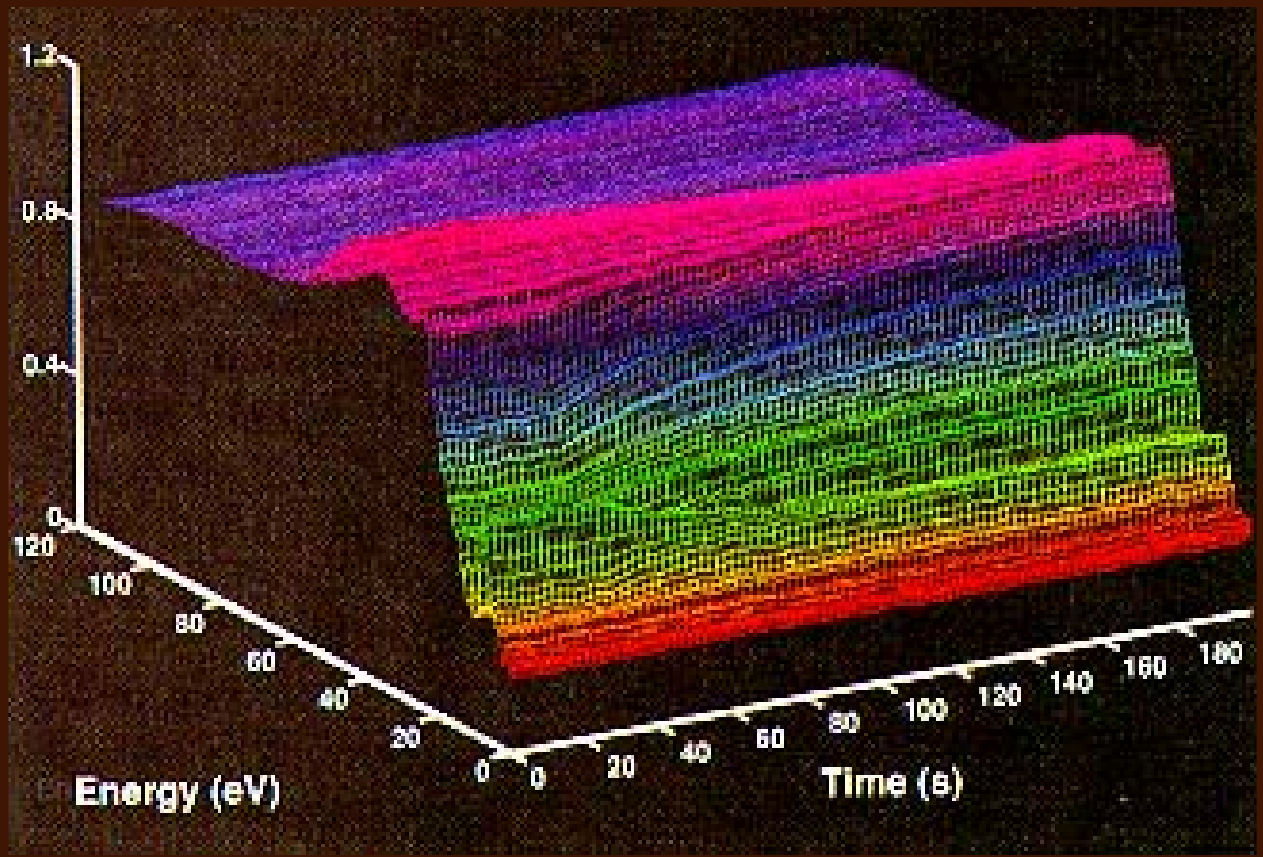

Descoberta de produtos de interesse, baseada em análise de padrões em bancos de dados (Weinstein et al., 97)

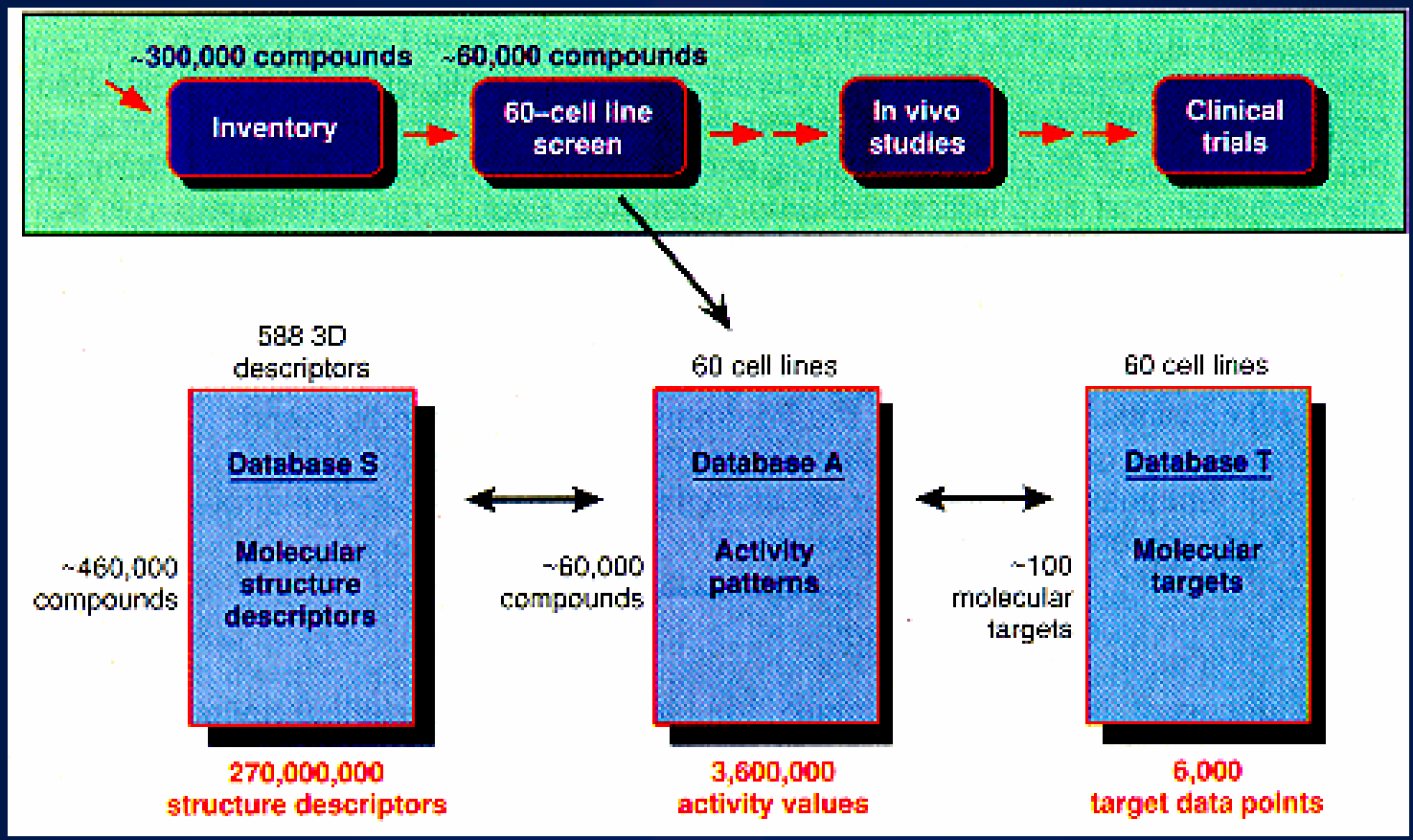

CHEMICAL PHYSICS

Polymorphic Phase Transitions in Liquids and Glasses

Peter H. Poole, Tor Grande, C. Austen Angell, Paul F. McMillan

At low temperatures, the thermodynamic equilibrium state of a pure substance is an ordered crystal. The crystalline portion of the pressure-temperature phase diagram is usually subdivided among several chemically identical but thermodynamically distinct polymorphs (*1*). Diamond and graphite are well-known examples. Such polymorphism is not restricted to crystals. Above the triple point, in the regimes of liquid and gas, distinct disordered phases are observed (see figure). Above the liquid-gas critical temperature T_c, these states merge into a single "fluid" phase. In this sense, the liquid and gas states can be regarded as "polymorphs" of the disordered fluid state (*2*).

The laws of thermodynamics permit the liquid region of the phase diagram for a pure substance to be subdivided into distinct phases (*3*). The coexistence of two distinct liquids is common in multicomponent chemical systems and also in liquid crystals, where composition and molecular orientation are the respective order parameters. However, "liquid polymorphism" for a pure, isotropic substance does not fall within our common experience. The usual microscopic picture of a liquid as a dynamic system with constantly rearranging molecular configurations makes it difficult to envisage distinct liquid phases, each with the same composition but with different thermodynamic properties and local structure. However, recent studies have revealed rich thermodynamic behaviors in a number of liquids that point to the occurrence of multiple liquid phases distinguished by density, not chemical composition. These results have implications for liquid and glass science, as well as for the thermodynamics of systems with fixed composition.

If liquid-liquid (L-L) phase transitions can occur for pure, isotropic substances, why are they not commonly observed? First, because the density will generally be an appropriate order parameter for such transitions, the exploration of a wide range of pressure and temperature may be required for their detection.

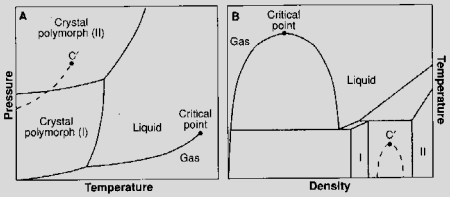

Schematic phase diagram of a pure substance exhibiting a liquid-liquid phase transition. (**A**) Solid lines locate the coexistence lines between the liquid, gas, and two crystal polymorphs. The liquid-gas coexistence line terminates in the critical point. The dashed line is the coexistence line for a liquid-liquid phase transition in the supercooled liquid, terminating in a critical point C′. (**B**) Projection of the lines given in (A) into the plane of temperature and density.

Second, the likely temperature range of L-L transitions must be considered. Because both phases are liquid, the changes in energy, entropy, and density across the transition at a given temperature will be much smaller than those for the liquid-gas transition. The resulting L-L coexistence curve should then be much narrower, and should terminate at a much lower temperature, than the liquid-gas coexistence curve. Moreover, the freezing temperature is typically less than T_c only by a factor of 2 to 4, so that most L-L transitions will be found below the crystal-liquid coexistence line; that is, they are most likely to be metastable transitions observed in the supercooled liquid state and may be obscured by crystal nucleation.

Third, even when crystal nucleation is avoided, a supercooled liquid cannot be studied in internal equilibrium to arbitrarily low temperatures, because of the dramatic increase in structural relaxation time τ. When τ exceeds the experimental observation time, the liquid properties are no longer observed in equilibrium, and the system has passed into the glassy state. Thus, a L-L transition in a supercooled liquid may also be obscured by the glass transition.

With these limitations in mind, what are the possibilities for observing liquid polymorphism? Among the most promising candidates to date are liquids having open molecular coordination environments at low pressure. Notably, these include liquids with a locally tetrahedral molecular structure, such as Si, Ge, C, SiO_2, GeO_2, and H_2O itself. For liquid Si, observation of a first-order glass-to-liquid transition, consistent with an underlying L-L transition, has been reported in flash-heating experiments (*4*) and computer simulations (*5*). For H_2O (*6*), SiO_2 (*7*), and GeO_2 (*8*), liquid polymorphism is suggested from glass studies at low temperatures. In all three cases, abrupt changes in density and glass structure with changing pressure closely resemble behavior associated with first-order phase transitions and have been described as "polyamorphic", that is, amorphous solid analogs of crystalline polymorphism (*9*). Although a glass is not an equilibrium thermodynamic state, if its behavior parallels that of the corresponding supercooled liquid, then the observation of a polyamorphic transition in a glass indicates the existence of distinct liquid states.

Theoretical and computer simulation studies also provide evidence for polymorphism in tetrahedral liquids. At the critical point of an L-L transition, response functions, such as the isothermal compressibility K_T, will diverge. On approaching this criticality from high temperatures, there will be a regime in which K_T exhibits a maximum, which is augmented on approach to T_c. Computer simulations of liquid H_2O (*10*) and SiO_2 (*11*) display K_T maxima that grow as T decreases. For H_2O, rapid crystal nucleation has so far precluded an experimental test of this prediction, but experiments on liquid SiO_2 (or, more conveniently, its structural analog BeF_2) at high pressures and temperatures should be feasible.

An intriguing report of liquid polymorphism has been recorded for the multicomponent system Y_2O_3-Al_2O_3 (*12*). During the quenching of melts with several Y/Al ratios, two coexisting glasses were obtained that were chemically identical but had different density and molecular structure. In this case, although the system could un-

P. H. Poole is in the Department of Applied Mathematics, University of Western Ontario, London, Ontario N6A 5B7, Canada. E-mail: poole@yorick.apmaths.uwo.ca. T. Grande is in the Department of Inorganic Chemistry, Norwegian University of Science and Technology, N-7034 Trondheim, Norway. C. A. Angell and P. F. McMillan are in the Department of Chemistry, Arizona State University, Tempe, AZ 85287, USA.

"...what are the possibilities for observing liquid polymorphism? Among the most promising candidates are...", *porém*, em macromoléculas, transições L-L foram observadas há quase trinta anos (Boyer, 70)